THE JOURNAL OF PHYSICAL CHEMISTRY Letters

Letter

pubs.acs.org/JPCL

Ultrafast Photoprotecting Sunscreens in Natural Plants

Lewis A. Baker,[†,‡] Michael D. Horbury,[†] Simon E. Greenough,[†,#] Florent Allais,[¶,§,∥] Patrick S. Walsh,[⊥] Scott Habershon,[†,‡] and Vasilios G. Stavros*[,†]

[†]Department of Chemistry and [‡]Centre for Scientific Computing, University of Warwick, Gibbet Hill Road, Coventry CV4 7AL, United Kingdom

[¶]Chaire Agro-Biotechnologies Industrielles (ABI), AgroParisTech, F-51100 Reims, France

[§]UMR GMPA, AgroParisTech, INRA, F-78850 Thiverval-Grignon, France

[∥]UMR IJPB, AgroParisTech, INRA, F-78026 Versailles, France

[⊥]Department of Chemistry, Purdue University, West Lafayette, Indiana 47907-2084, United States

Supporting Information

ABSTRACT: We explore the ultrafast photoprotective properties of a series of sinapic acid derivatives in a range of solvents, utilizing femtosecond transient electronic absorption spectroscopy. We find that a primary relaxation mechanism displayed by the plant sunscreen sinapoyl malate and other related molecular species may be understood as a multistep process involving internal conversion of the initially photoexcited $1^1\pi\pi^*$ state along a trans−cis photoisomerization coordinate, leading to the repopulation of the original trans ground-state isomer or the formation of a stable cis isomer.

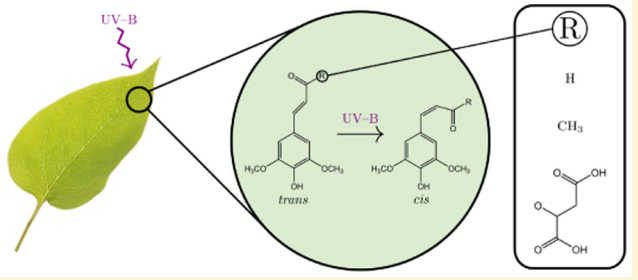

Ultraviolet radiation (UV) that reaches the Earth's surface has an extensive impact on the biosphere.[1,2] Of particular interest are the high-energy components of the solar UV spectrum, UV-B (280−315 nm), and the shorter wavelengths of the UV-A region (<340 nm), collectively referred from hereon as "UV-R". In plants, UV-R acts as a signal transducer for numerous processes including immune response, plant morphology, and the phenylpropanoid pathway.[2,3] Deleterious effects of this radiation exposure to organisms are widely known, for example, reduction of photosynthesis, growth inhibition, and susceptibility to pathogens.[4,5] As such, plants synthesize and deposit UV-absorbing phenolic compounds in epidermal tissues via the phenylpropanoid pathway to protect against overexposure to UV radiation.[2,3]

Specifically, studies of gene mutations in the plant *Arabidopsis thaliana*, a member of the *Brassicaceae* family, have found that the phenylpropanoid pathway could be disrupted such that the concentrations of sinapate esters present in the epidermal layers of the plant are reduced, rendering the plant hypersensitive to UV-R exposure.[6−11] Such experiments therefore point to sinapate esters as being the likely class of UV-R screening molecules used by *Brassicaceae* plants. Sinapate esters are derivatives of sinapic acid (SA) and closely related to sinapoyl malate (SM), which has been identified to be the dominant constituent deposited in the upper epidermis of *Arabidopsis* plant leaves.[7,8,11] The interesting question that remains in light of this is, *how* do these molecules provide UV-R photoprotection?

Previous work in characterizing the photophysical properties of cinnamates,[12−19] a set of molecules closely related to the sinapates, identified a variety of relaxation pathways after an initial photoexcitation to a $1^1\pi\pi^*$ state. In particular, relaxation through internal conversion (IC), mediated by trans−cis isomerization,[12−16] or IC to a long-lived $1^1n\pi^*$ state[17,20−24] has been suggested as a viable relaxation mechanism. In SA, similar studies suggest that IC along an aborted trans−cis isomerization of the aliphatic C═C bond couples the excited state to the ground state.[25] Recent vibrationally resolved UV spectroscopy measurements of SA, SM, and the simplest derivative methyl sinapate (MS), suggest that along this series, SM is unique in having an inherently broad absorption spectrum even under jet-cooled gas-phase conditions exhibiting an efficient, nonradiative energy dissipation mechanism that may be responsible for the biological selectivity of SM as a UV-R photoprotective sunscreen molecule in plants.[26] These studies provide a solid foundation to build upon in understanding the underlying photodynamics of the sinapate ester derivatives presented here.

In this Letter, we use femtosecond pump−probe transient electronic (UV−visible) absorption spectroscopy (TEAS) to probe the ultrafast energy relaxation mechanism of SA, MS, and SM in the solution phase. We complement these measurements with continuous-wave UV irradiation studies to elucidate long-lived photoproducts. We present evidence to suggest that photoexcited SA, MS, and SM relax by IC to the ground

Received: November 5, 2015
Accepted: December 10, 2015
Published: December 10, 2015

DOI: 10.1021/acs.jpclett.5b02474
J. Phys. Chem. Lett. 2016, 7, 56−61

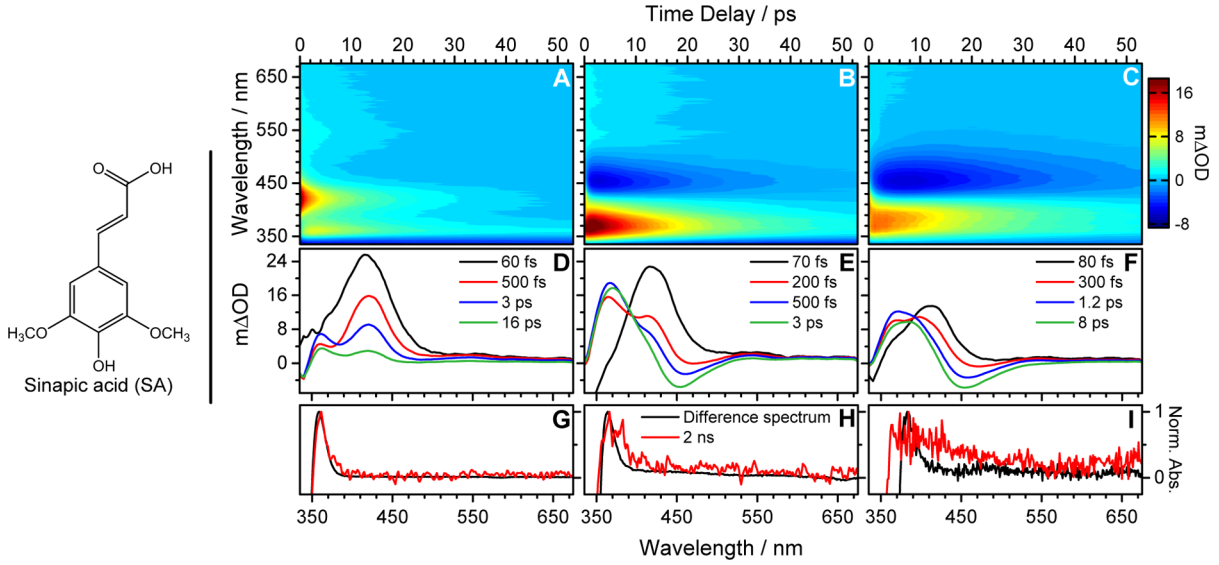

Figure 1. TAS for SA in solution with dioxane (A), ACN (B), and methanol (C) in the form of a color map indicating the change in optical density (ΔOD). Selected slices of the TAS at specific delay times for SA−dioxane (D), SA−ACN (E), and SA−methanol (F). Complementary UV irradiation difference spectra for SA−dioxane (G), SA−ACN (H), and SA−methanol (I) are shown as a black line in comparison to the absorption spectrum at the maximum available pump−probe time delay of 2 ns (red line).

electronic state via a trans−cis isomerization of the aliphatic C═C bond.

The TEAS setup[27,28] used throughout this work employed ∼320−330 nm, 1−2 mJ cm^{-2} pump pulses with probe pulses drawn from a broad-band white-light continuum (335−675 nm), with polarization set to the magic angle (54.7°) relative to the pump pulses. Transient absorption spectra (TAS) were taken of 1 mM SA (≥98%, Sigma-Aldrich), MS, and SM (synthesized as described previously[29,30]), in solution with either the nonpolar aprotic solvent dioxane (≥99%, Fisher Scientific), the polar aprotic solvent acetonitrile (ACN; ≥ 99%, Sigma-Aldrich), or the polar protic solvent methanol (≥99.6%, Sigma-Aldrich) for a range of pump−probe time delays, Δt, up to a maximum of 2 ns. Each molecule was excited at its UV-R absorption maximum (see the Supporting Information (SI)). All TAS were chirp-corrected using the KOALA package,[31] and reported lifetimes were determined using a global fitting procedure[27,32] with uncertainties reported to a 95% confidence interval (2σ) using asymptotic standard errors; see the SI for details.

Continuous-wave UV irradiation studies were performed on all molecules using the following procedure. A static UV−visible spectrum of each sample was taken (Cary 300 spectrometer), to obtain a "before" spectrum. Samples were then irradiated with continuous-wave radiation from an arc lamp (OBB, Tunable KiloArc) for 10 min. The central wavelength used for irradiation was the same as the pump wavelength used in the TEAS measurements. The bandwidth was set to 10 nm with a power of 3 W. A second UV−visible spectrum was taken following irradiation, referred to as the "after" spectrum. The before spectrum was subtracted from the after spectrum, resulting in the reported "difference spectrum".

Considering first the biological precursor, SA, in solution with dioxane, ACN, or methanol, the TAS are shown in Figure 1 for photoexcitation at 325, 323, and 318 nm, respectively. For SA−dioxane (Figure 1A), the TAS is dominated by three features. First is an intense absorption centered at ∼420 nm, which decays away to the baseline by ∼50 ps. Second, there is a broad absorption spanning the spectral region of ∼420−650 nm. Finally, a negative signal is observed below ∼350 nm. Because photoexcitation at around ∼320 nm (∼4 eV) promotes a $1^1\pi\pi^* \leftarrow S_0$ transition,[26] the first two features are attributed to excited-state absorption (ESA) of the $1^1\pi\pi^*$ state (i.e., $S_n \leftarrow 1^1\pi\pi^*$). The negative feature, which grows in with increasing pump−probe time delays, with the decay of the ESA, is assigned to a ground-state bleach (GSB) through comparison with the static UV−visible absorption spectrum (see the SI), which does not fully recover at the maximum available pump−probe time delay of 2 ns. The TAS for SA−ACN and SA−methanol (Figure 1B and C, respectively) are also dominated by the three features seen in the SA−dioxane TAS with these addenda: the intense absorption of the $1^1\pi\pi^*$ ESA is blue-shifted, centered instead on ∼370 nm, and an additional feature is observed; there is also a strong negative signal centered at around ∼460 nm that we attribute to stimulated emission.[26,33]

Quantitative insight into the dynamical processes observed in the TAS can be obtained by employing a global fitting procedure (see the SI).[27,32] The lifetimes of the available processes are summarized in Table 1 for all of the systems

Table 1. Summary of the Lifetimes of Dynamical Processes of SA, MS, and SM

	dioxane	ACN	methanol
		SA	
τ_1/fs	93 ± 17	52 ± 5	572 ± 87
τ_2/ps	0.90 ± 0.19	0.57 ± 0.04	3.79 ± 0.72
τ_3/ps	12.2 ± 1.1	17.0 ± 0.66	25.5 ± 1.6
		MS	
τ_1/fs	115 ± 49	53 ± 5	647 ± 114
τ_2/ps	1.32 ± 0.16	0.54 ± 0.05	4.26 ± 0.90
τ_3/ps	12.8 ± 1.3	18.0 ± 0.8	24.2 ± 1.5
		SM	
τ_1/fs	119 ± 28	51 ± 4	619 ± 101
τ_2/ps	1.62 ± 0.15	0.63 ± 0.04	4.81 ± 0.77
τ_3/ps	22.4 ± 1.9	27.3 ± 0.77	33.5 ± 1.7

DOI: 10.1021/acs.jpclett.5b02474
J. Phys. Chem. Lett. 2016, 7, 56−61

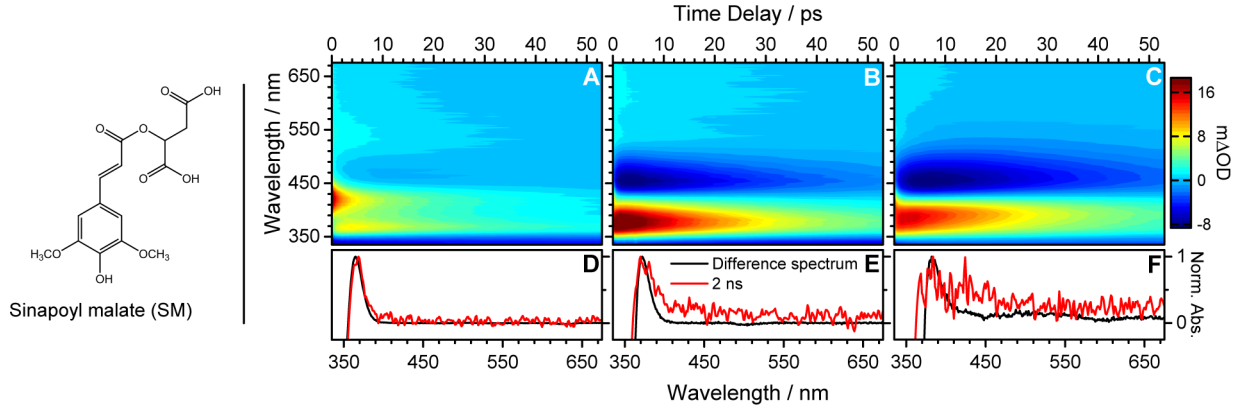

Figure 2. TAS for SM in solution with dioxane (A), ACN (B), and methanol (C) in the form of a color map indicating the change in optical density (ΔOD). Complementary UV irradiation difference spectra for SM−dioxane (D), SM−ACN (E), and SM−methanol (F) are shown as a black line in comparison to the absorption spectrum at the maximum available pump−probe time delay of 2 ns (red line).

studied herein, and we return to this table throughout our ensuing discussion. Following this, continuous-wave irradiation was used to investigate the incomplete GSB recovery and assist in our analysis of these dynamical processes. The resulting difference UV−visible spectra are shown in the bottom panels of Figure 1 (black lines), overlaid with the absorption spectrum obtained for Δt = 2 ns from the corresponding TAS (red lines). For SA−dioxane, the difference spectrum and the Δt = 2 ns spectrum (Figure 1G) match closely, with a positive absorption appearing at ∼370 nm in both spectra. This ∼370 nm absorption is also seen in SA−ACN, and its red-wavelength shoulder is spectrally broadened. Finally, for SA−methanol, there are large discrepancies between the difference spectrum and the absorption spectrum obtained for Δt = 2 ns (Figure 1I). A ∼20 nm "gap" between the two absorption features is observed. Once again, there is a shoulder to the red of the absorption feature in the Δt = 2 ns spectrum, which appears broader than that seen in SA−dioxane and SA−ACN. We note that the results for MS closely agree with those of SA and are presented in the SI and Table 1 for completeness.

We now consider the biological sunscreen deposited in the upper epidermis of plant leaves, SM. The TAS are shown in Figure 2A−C for SM-dioxane, SM−ACN, and SM−methanol for photoexcitation at 329, 328, and 326 nm, respectively. As described for both SA and MS studies, similar solvent-dependent spectral features are observed in the TAS. Once again employing a global fitting procedure, we determine the lifetimes of the dynamical processes, and these are summarized in Table 1. Continuous-wave studies also reveal similar patterns as those observed for SA and MS (Figures 2D−F), specifically, an increasing shoulder appearing to the red of the absorption feature at ∼370 nm in the more protic and hydrogen-bonding solvent methanol.

We now discuss the implications with regards to photoprotection, drawing on the different aspects of the experimental results. First, considering the continuous-wave irradiation studies, we note very good agreement between the difference spectrum and the Δt = 2 ns spectrum for SA, MS, and SM in the aprotic, weakly hydrogen bonding solvent dioxane. In these measurements, the trans isomer and any photoproduct will have different static UV−visible spectra, and as such, any appreciable formation of photoproducts can be identified. An intense positive peak centered at ∼370 nm is attributed to a long-lived photoproduct, which we assign to be the cis isomer of each molecule, drawing confidence from the observation of photoisomerization in similar molecules.[16,17] This feature is also seen for SA, MS, and SM in ACN and, to a lesser extent, methanol. In addition, a weak absorption is observed, convoluted with the ∼370 nm peak, which we have referred to as the red-wavelength shoulder. In ACN, an aprotic, mild hydrogen bonding solvent, for all three molecules, we observe a broadening of this red-wavelength shoulder. In methanol, a protic strongly hydrogen bonding solvent, the three molecules display this signal broadening as with ACN, but the absorption feature of the difference spectrum is spectrally red-shifted ∼20 nm relative to the Δt = 2 ns spectrum for all three molecules. The absorption feature in the Δt = 2 ns spectrum has characteristics similar to the UV−visible absorption spectrum of the SA radical.[25] We attribute the disparity seen for *all* methanol measurements (and to some extent in ACN) between the Δt = 2 ns absorption spectrum and the difference spectrum to two processes: (1) a two-photon (at least) ionization process that generates the radical (see the power dependency measurements in the SI for SA as exemplar)[34−36] and (2) possible triplet-state absorption given the characteristic "tail" in the absorption toward the red end of the TAS.[37] We suggest that (1) arises due to methanol's (and again, to some extent ACN) apparent propensity to alter the electronic structure of the molecules through perturbative interactions.

Through due consideration of the data provided by the TEAS measurements, drawing on ab initio calculations on isolated "gas-phase" hydroxycinnamic acids[38] and experimental results on related systems,[26,34] we attempt to rationalize the dynamical processes in operation. We do however note that additional theory is required to fully comprehend the dynamical processes evidently in operation. Following excitation to the $1^1\pi\pi^*$ state by the pump pulse, we propose that SA, MS, and SM undergo numerous processes that are convoluted together and described by the lifetimes τ_1 and τ_2, thus making distinct assignment of any one process with a lifetime difficult. In particular, we suggest that a coherent artifact of the instrument response function and an evolution out of the Franck−Condon window contribute to τ_1. Along with any solvent rearrangement, IC ensues from this state to the intermediary $2^1\pi\pi^*$ state via a $1^1\pi\pi^*/2^1\pi\pi^*$ conical intersection (CI), which we suggest contributes to the lifetime τ_2. The time scale for these processes sensibly compares with previous dynamical studies in related molecular systems.[25,33,35,37,39−41] Both of these lifetimes will inevitably be effected by the formation of the radical species (see Table 1). From here, isomerization may occur along the

DOI: 10.1021/acs.jpclett.5b02474
J. Phys. Chem. Lett. 2016, 7, 56−61

$2^1\pi\pi^*$ state to generate the cis isomer in S_0, mediated through a $2^1\pi\pi^*/S_0$ CI, with the remaining population reverting back to the original ground-state trans isomer. These final steps account for the lifetime τ_3. The overall relaxation dynamics are depicted in the schematic shown in Figure 3. An alternative relaxation

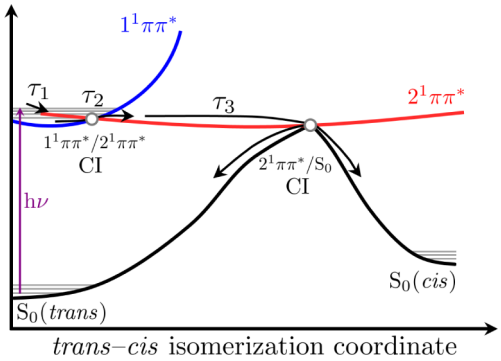

Figure 3. Schematic of the relaxation scheme proposed in this work adapted from the calculated potential energy surfaces for similar systems;[38] a vertical excitation to the $1^1\pi\pi^*$ state and IC to a $2^1\pi\pi^*$ state in the adiabatic limit before nonadiabatic transfer to the ground electronic (S_0) state, with associated time scales τ_1, τ_2, and τ_3 as discussed in the text. The $1^1n\pi^*$ state has been omitted for simplicity. Note that an alternative relaxation mechanism involves dynamics along a single excited ($1^1\pi\pi^*$) state; see the main text for details.

mechanism to that proposed in Figure 3 consistent with the data presented should be noted. The dynamics may ensue from the $1^1\pi\pi^*$ to the S_0 without the $2^1\pi\pi^*$ intermediary state. In this case, τ_1 and τ_2 would be considered relaxation along a single potential energy surface (which likely will be convoluted with numerous processes; see above) before coupling back to the S_0 via a $1^1\pi\pi^*/S_0$ CI on the time scale of τ_3.[25]

We suggest that the stimulated emission observed for SA, MS, and SM in ACN and methanol is likely to originate from population on the $2^1\pi\pi^*$ (or $1^1\pi\pi^*$ considering an alternative mechanism). This assignment is given for the following reasons. The onset of the stimulated emission signals is from $\Delta t \approx 100$ fs onward and last beyond $\Delta t > 30$ ps, which is on the time scale of τ_3; see Figure 1E and F. The signals are spectrally broad,[25] which is consistent with a disperse excited-state population along the plateau of the $2^1\pi\pi^*$ (or $1^1\pi\pi^*$) potential energy surface. No stimulated emission is observed for dioxane measurements, which we suggest is due to the much larger, positive-going, ESA convoluted with any stimulated emission. Finally, we note the very good agreement between the spectral location of the stimulated emission in SA and SM and previous fluorescence measurements.[26]

Some general remarks are needed regarding the lifetimes of the dynamical processes given in Table 1 and how these are influenced by additional factors not included in the schematic of Figure 3. First, it is a limitation of the global fitting procedure that all lifetimes correspond to processes that start instantaneously (i.e., nonsequential dynamics). This has the effect of "blurring" the onset of one process with the onset of another. Ultimately, this means that each lifetime will also capture some of the preceding and/or proceeding dynamics, making the absolute assignment of a lifetime with any one process very difficult.[32,42] Second, it is evident that all of the lifetimes measured for methanol are appreciably longer than those measured in dioxane and ACN, which we attribute to the formation of the radical (and the associated solvated electron; see the SI).

We close with a comparison between the present solution-phase measurements and those recently obtained in the gas phase, focusing on SA as this system demonstrates quite notable differences.[26] Sharp features in the resonant two-photon ionization spectrum for SA implies an initial excited-state lifetime on the order of picoseconds, in stark contrast to the SA–dioxane results obtained herein of ~100 fs. One would anticipate observing similar time scales between the weakly perturbing nonpolar dioxane solvent and the gas phase. However, in addition to the mild perturbations induced by the solvent, SA exists as a dimer in dioxane, which will of course influence its electronic structure (see the SI for the IR spectrum).[43,44] In ACN and methanol, the hydrogen bonds between dimers are broken; however, the strong perturbations to the electronic structure by these solvents (vide supra) will inevitably lead to larger deviations between the gas- and solution-phase studies. Importantly, the differences between these two phases serve to highlight the crucial role of both solvent dynamics– and structure–dynamics–function relationships. For example, if either the $1^1n\pi^*$ (as suggested to be involved in the gas phase[26]) or $2^1\pi\pi^*$ state has charge-transfer character, it will further influence the energy difference between these two states and hence the excited-state dynamics due to solvent stability effects.[26]

In summary, we have explored the photoprotection mechanisms in operation in SA, MS, and the plant sunscreen SM. In all three systems, excited-state relaxation occurs on an ultrafast time scale, involving, in part, IC from $1^1\pi\pi^* \rightarrow 2^1\pi\pi^* \rightarrow S_0$, mediated by the appropriate $1^1\pi\pi^*/2^1\pi\pi^*$ and $2^1\pi\pi^*/S_0$ CIs. Importantly, at the $2^1\pi\pi^*/S_0$ CI, the photoexcited molecule can either re-form the original ground-state trans isomer or generate the cis isomer. We also suggest a combination of other processes in operation, notably the formation of a radical species and possibly intersystem crossing. Crucially, however, and with the exception of the radical species that is generated through consequence of the experiment itself (at least a two-photon absorption process that is unlikely to occur in nature), the present work serves to highlight the efficiency in which the plant sunscreen, SM, is able to undergo ultrafast relaxation in order to bypass the deleterious effects of UV radiation in the biosphere. This study also further highlights that there may be other reasons why SM is selected as a sunscreen molecule in plants, given that there is little difference in the excited-state dynamics between the biological precursor (SA) through to plant sunscreen (SM) in the solution phase.

■ ASSOCIATED CONTENT

Supporting Information

The Supporting Information is available free of charge on the ACS Publications website at DOI: 10.1021/acs.jpclett.5b02474.

TAS and difference spectra of MS in dioxane, ACN, and methanol; UV–visible absorption spectra of MS, SA, and SM in a range of solvents; TEAS experimental, global fitting, and asymptotic standard error details; decay associated spectra, fitting residuals, and infrared spectra of SA; selected spectra of MS and SM for specific delay times; and power-dependent measurements for SA (PDF)

DOI: 10.1021/acs.jpclett.5b02474
J. Phys. Chem. Lett. 2016, 7, 56–61

AUTHOR INFORMATION

Present Address

[#]S.E.G.: Department of Chemistry, University of Sheffield, Sheffield S3 7HF, United Kingdom.

Notes

The authors declare no competing financial interest.

ACKNOWLEDGMENTS

The authors are grateful to Prof. Peter J. Sadler (University of Warwick) for the use the KiloArc and Prof. Alison Rodger (University of Warwick) for the use of the infrared spectrometer. The authors also thank Prof. Timothy S. Zwier (Purdue University) and Dr. Tolga N. V. Karsili (Technische Universität München) for useful discussions. L.A.B. thanks the Engineering and Physical Sciences Research Council (EPSRC) for providing a studentship under Grant EP/F500378/1 through the Molecular Organisation and Assembly in Cells Doctoral Training Centre and the Centre for Scientific Computing at the University of Warwick for providing computational resources. M.D.H. thanks the University of Warwick for an EPSRC studentship. S.E.G. thanks the Warwick Institute of Advanced Study for postdoctoral funding. V.G.S. thanks the EPSRC for an equipment grant (EP/J007153) and the Royal Society for a University Research Fellowship.

REFERENCES

(1) Paul, N. D.; Gwynn-Jones, D. Ecological Roles of Solar UV Radiation: Towards an Integrated Approach. *Trends Ecol. Evol.* **2003**, *18*, 48−55.

(2) Caldwell, M. M.; Bornman, J. F.; Ballaré, C. L.; Flint, S. D.; Kulandaivelu, G. Terrestrial Ecosystems, Increased Solar Ultraviolet Radiation, and Interactions with Other Climate Change Factors. *Photochem. Photobiol. Sci.* **2007**, *6*, 252−266.

(3) Jenkins, G. I. Signal Transduction in Responses to UV-B Radiation. *Annu. Rev. Plant Biol.* **2009**, *60*, 407−431.

(4) Tevini, M.; Teramura, A. H. UV-B Effects on Terrestrial Plants. *Photochem. Photobiol.* **1989**, *50*, 479−487.

(5) Frohnmeyer, H.; Staiger, D. Ultraviolet-B Radiation-Mediated Responses in Plants. Balancing Damage and Protection. *Plant Physiol.* **2003**, *133*, 1420−1428.

(6) Li, J.; Ou-Lee, T.-M.; Raba, R.; Amundson, R. G.; Last, R. L. Arabidopsis Flavonoid Mutants Are Hypersensitive to UV-B lrradiation. *Plant Cell* **1993**, *5*, 171−179.

(7) Chapple, C. C. S.; Vogt, T.; Elliis, B. E.; Somerville, C. R. An Arabidopsis Mutant Defective in the General Phenylpropanoid Pathway. *Plant Cell* **1992**, *4*, 1413−1424.

(8) Ruegger, M.; Chapple, C. Mutations That Reduce Sinapoylmalate Accumulation in *Arabidopsis Thaliana* Define Loci with Diverse Roles in Phenylpropanoid Metabolism. *Genetics* **2001**, *159*, 1741−1749.

(9) Bieza, K.; Lois, R. An Arabidopsis Mutant Tolerant to Lethal Ultraviolet-B Levels Shows Constitutively Elevated Accumulation of Flavonoids and Other Phenolics. *Plant Physiol.* **2001**, *126*, 1105−1115.

(10) Milkowski, C.; Baumert, A.; Schmidt, D.; Nehlin, L.; Strack, D. Molecular Regulation of Sinapate Ester Metabolism in *Brassica Napus*: Expression of Genes, Properties of the Encoded Proteins and Correlation of Enzyme Activities with Metabolite Accumulation. *Plant J.* **2004**, *38*, 80−92.

(11) Fraser, C. M.; Chapple, C. The Phenylpropanoid Pathway in Arabidopsis. *Arabidopsis Book* **2011**, *9*, e0152.

(12) Lewis, F. D.; Quillen, S. L.; Elbert, J. E.; Schneider, S.; Geiselhart, P. The Singlet States of Methyl Cinnamate and Methyl Indenoate. *J. Photochem. Photobiol., A* **1989**, *47*, 173−179.

(13) Pattanaargson, S.; Limphong, P. Stability of Octyl Methoxycinnamate and Identification of Its Photo-Degradation Product. *Int. J. Cosmet. Sci.* **2001**, *23*, 153−160.

(14) Promkatkaew, M.; Suramitr, S.; Karpkird, T. M.; Namuangruk, S.; Ehara, M.; Hannongbua, S. Absorption and Emission Spectra of Ultraviolet B Blocking Methoxy Substituted Cinnamates Investigated Using the Symmetry-Adapted Cluster Configuration Interaction Method. *J. Chem. Phys.* **2009**, *131*, 224306.

(15) Singh, T. S.; Mitra, S.; Chandra, A.; Tamai, N.; Kar, S. A Combined Experimental and Theoretical Study on Photoinduced Intramolecular Charge Transfer in *Trans*-Ethyl *p*-(Dimethylamino)-cinamate. *J. Photochem. Photobiol., A* **2008**, *197*, 295−305.

(16) Miyazaki, Y.; Inokuchi, Y.; Akai, N.; Ebata, T. Direct Spectroscopic Evidence of Photoisomerization in Para-Methoxy Methylcinnamate Revealed by Low-Temperature Matrix-Isolation FTIR Spectroscopy. *J. Phys. Chem. Lett.* **2015**, *6*, 1134−1139.

(17) Karpkird, T. M.; Wanichweacharungruang, S.; Albinsson, B. Photophysical Characterization of Cinnamates. *Photochem. Photobiol. Sci.* **2009**, *8*, 1455−1460.

(18) Shimada, D.; Kusaka, R.; Inokuchi, Y.; Ehara, M.; Ebata, T. Nonradiative Decay Dynamics of Methyl-4-Hydroxycinnamate and Its Hydrated Complex Revealed by Picosecond Pump-Probe Spectroscopy. *Phys. Chem. Chem. Phys.* **2012**, *14*, 8999−9005.

(19) Gromov, E. V.; Burghardt, I.; Köppel, H.; Cederbaum, L. S. Impact of Sulfur Vs Oxygen on the Low-Lying Excited States of *Trans*-*p*-Coumaric Acid and *Trans*-*p*-Coumaric Thio Acid. *J. Phys. Chem. A* **2005**, *109*, 4623−4631.

(20) Kuramochi, H.; Takeuchi, S.; Tahara, T. Ultrafast Structural Evolution of Photoactive Yellow Protein Chromophore Revealed by Ultraviolet Resonance Femtosecond Stimulated Raman Spectroscopy. *J. Phys. Chem. Lett.* **2012**, *3*, 2025−2029.

(21) Tan, E. M. M.; Hilbers, M.; Buma, W. J. Excited-State Dynamics of Isolated and Microsolvated Cinnamate-Based UV-B Sunscreens. *J. Phys. Chem. Lett.* **2014**, *5*, 2464−2468.

(22) de Groot, M.; Gromov, E. V.; Köppel, H.; Buma, W. J. High-Resolution Spectroscopy of Methyl 4-Hydroxycinnamate and Its Hydrogen-Bonded Water Complex. *J. Phys. Chem. B* **2008**, *112*, 4427−4434.

(23) Smolarek, S.; Vdovin, A.; Perrier, D. L.; Smit, J. P.; Drabbels, M.; Buma, W. J. High-Resolution Excitation and Absorption Spectroscopy of Gas-Phase *p*-Coumaric Acid: Unveiling an Elusive Chromophore. *J. Am. Chem. Soc.* **2010**, *132*, 6315−6317.

(24) Tan, E. M. M.; Amirjalayer, S.; Bakker, B. H.; Buma, W. J. Excited State Dynamics of Photoactive Yellow Protein Chromophores Elucidated by High-Resolution Spectroscopy and *Ab Initio* Calculations. *Faraday Discuss.* **2013**, *163*, 321−340.

(25) Vengris, M.; Larsen, D. S.; van der Horst, M. A.; Larsen, O. F. A.; Hellingwerf, K. J.; van Grondelle, R. Ultrafast Dynamics of Isolated Model Photoactive Yellow Protein Chromophores: "Chemical Perturbation Theory" in the Laboratory. *J. Phys. Chem. B* **2005**, *109*, 4197−4208.

(26) Dean, J. C.; Kusaka, R.; Walsh, P. S.; Allais, F.; Zwier, T. S. Plant Sunscreens in the UV-B: Ultraviolet Spectroscopy of Jet-Cooled Sinapoyl Malate, Sinapic Acid, and Sinapate Ester Derivatives. *J. Am. Chem. Soc.* **2014**, *136*, 14780−14795.

(27) Baker, L. A.; Horbury, M. D.; Greenough, S. E.; Coulter, P. M.; Karsili, T. N. V.; Roberts, G. M.; Orr-Ewing, A. J.; Ashfold, M. N. R.; Stavros, V. G. Probing the Ultrafast Energy Dissipation Mechanism of the Sunscreen Oxybenzone after UVA Irradiation. *J. Phys. Chem. Lett.* **2015**, *6*, 1363−1368.

(28) Greenough, S. E.; Roberts, G. M.; Smith, N. A.; Horbury, M. D.; McKinlay, R. G.; Żurek, J. M.; Paterson, M. J.; Sadler, P. J.; Stavros, V. G. Ultrafast Photo-Induced Ligand Solvolysis of *Cis*-$[Ru(bipyridine)_2(nicotinamide)_2]^{2+}$: Experimental and Theoretical Insight into Its Photoactivation Mechanism. *Phys. Chem. Chem. Phys.* **2014**, *16*, 19141−19155.

(29) Allais, F.; Martinet, S.; Ducrot, P.-H. Straightforward Total Synthesis of 2-*O*-Feruloyl-L-Malate, 2-*O*-Sinapoyl-L-Malate and 2-*O*-5-Hydroxyferuloyl-L-Malate. *Synthesis* **2009**, *2009*, 3571−3578.

(30) Quentin, M.; Allasia, V.; Pegard, A.; Allais, F.; Ducrot, P.-H.; Favery, B.; Levis, C.; Martinet, S.; Masur, C.; Ponchet, M.; et al.

DOI: 10.1021/acs.jpclett.5b02474
J. Phys. Chem. Lett. 2016, 7, 56−61

Imbalanced Lignin Biosynthesis Promotes the Sexual Reproduction of Homothallic Oomycete Pathogens. *PLoS Pathog.* **2009**, *5*, e1000264.
(31) Grubb, M. P.; Orr-Ewing, A. J.; Ashfold, M. N. R. KOALA: a Program for the Processing and Decomposition of Transient Spectra. *Rev. Sci. Instrum.* **2014**, *85*, 0641024.
(32) Chatterley, A. S.; West, C. W.; Stavros, V. G.; Verlet, J. R. R. Time-Resolved Photoelectron Imaging of the Isolated Deprotonated Nucleotides. *Chem. Sci.* **2014**, *5*, 3963−3975.
(33) Mataga, N.; Chosrowjan, H.; Taniguchi, S.; Hamada, N.; Tokunaga, F.; Imamoto, Y.; Kataoka, M. Ultrafast Photoreactions in Protein Nanospaces as Revealed by Fs Fluorescence Dynamics Measurements on Photoactive Yellow Protein and Related Systems. *Phys. Chem. Chem. Phys.* **2003**, *5*, 2454−2460.
(34) Foley, S.; Navaratnam, S.; McGarvey, D. J.; Land, E. J.; Truscott, T. G.; Rice-Evans, C. A. Singlet Oxygen Quenching and the Redox Properties of Hydroxycinnamic Acids. *Free Radical Biol. Med.* **1999**, *26*, 1202−1208.
(35) Vengris, M.; van Stokkum, I. H. M.; He, X.; Bell, A. F.; Tonge, P. J.; van Grondelle, R.; Larsen, D. S. Ultrafast Excited and Ground-State Dynamics of the Green Fluorescent Protein Chromophore in Solution. *J. Phys. Chem. A* **2004**, *108*, 4587−4598.
(36) Larsen, D. S.; van Stokkum, H. M.; Vengris, M.; van der Horst, M. A.; de Weerd, F. L.; Hellingwerf, K. J.; van Grondelle, R. Incoherent Manipulation of the Photoactive Yellow Protein Photocycle with Dispersed Pump-Dump-Probe Spectroscopy. *Biophys. J.* **2004**, *87*, 1858−1872.
(37) Horbury, M. D.; Baker, L. A.; Quan, W.-D.; Young, J. D.; Staniforth, M.; Greenough, S. E.; Stavros, V. G. Bridging the Gap Between the Gas Phase and Solution Phase: Solvent Specific Photochemistry in 4-*Tert*-Butylcatechol. *J. Phys. Chem. A* **2015**, DOI: 10.1021/acs.jpca.5b03621.
(38) Karsili, T. N. V.; Marchetti, B.; Ashfold, M. N. R.; Domcke, W. *Ab Initio* Study of Potential Ultrafast Internal Conversion Routes in Oxybenzone, Caffeic Acid, and Ferulic Acid: Implications for Sunscreens. *J. Phys. Chem. A* **2014**, *118*, 11999−12010.
(39) Castner, E. W., Jr.; Maroncelli, M.; Fleming, G. R. Subpicosecond Resolution Studies of Solvation Dynamics in Polar Aprotic and Alcohol Solvents. *J. Chem. Phys.* **1987**, *86*, 1090−1097.
(40) Owrutsky, J. C.; Raftery, D.; Hochstrasser, R. M. Vibrational Relaxation Dynamics in Solutions. *Annu. Rev. Phys. Chem.* **1994**, *45*, 519−555.
(41) Espagne, A.; Paik, D. H.; Changenet-Barret, P.; Martin, M. M.; Zewail, A. H. Ultrafast Photoisomerization of Photoactive Yellow Protein Chromophore Analogues in Solution: Influence of the Protonation State. *ChemPhysChem* **2006**, *7*, 1717−1726.
(42) Hockett, P. *Faraday Discuss.* **2013**, *163*, 513−543.
(43) Ge, M.; Zhao, H.; Wang, W.; Zhang, Z.; Yu, X.; Li, W. Terahertz Time-Domain Spectroscopy of Four Hydroxycinnamic Acid Derivatives. *J. Biol. Phys.* **2007**, *32*, 403−412.
(44) Chung, S.-K.; Osawa, T.; Kawakishi, S. Hydroxyl Radical-Scavenging Effects of Spices and Scavengers from Brown Mustard (Brassica nigra). *Biosci., Biotechnol., Biochem.* **1997**, *61*, 118−123.

DOI: 10.1021/acs.jpclett.5b02474
J. Phys. Chem. Lett. 2016, 7, 56−61